INTERNATIONAL JOURNAL OF AUTOMOTIVE AND MECHANICAL ENGINEERING
ISSN: 2229-8649 e-ISSN: 2180-1606
VOLUME 23, ISSUE 2, 2026, 13601 - 13616
DOI: https://doi.org/10.15282/ijame.23.2.2026.10.1029

RESEARCH ARTICLE

Thermal, mechanical, and sound absorption properties of sugarcane bagasse–rice husk hybrid polymer composites

Niresh Jayarajan[1]*, Tan Wei Hong[1], Tamilselvan Ganesan[2]

[1]Faculty of Mechanical Engineering & Technology, Universiti Malaysia Perlis (UniMAP), Pauh Putra Campus, 02600, Arau, Perlis, Malaysia
[2]Department of Mechanical Engineering, Mepco Schlenk Engineering College, Sivakasi, Tamil Nadu, India

Abstract - Natural fibre reinforced composites are explored more as sustainable alternatives to synthetic materials, but the challenge of obtaining a balance between thermal insulation, mechanical strength and acoustic absorption is still an important problem. This study evaluates the performance of hybrid composites with sugarcane bagasse (SCB) and rice husk (RH) in weight ratios of 100%, 70/30, 50/50 and 30/70 using thermoset resin matrix. Thermal conductivity was measured by Lee's Disc Method, the 100% RH sample obtained the lowest thermal conductivity of 0.03502 W/mK, which showed a good insulation performance. Mechanical characterization according to the standards of tensile strength and flexural strength of the samples in accordance with ASTM D3039, D790, and D256 showed that the 50/50 SCB-RH composite had the highest tensile strength (80.1 MPa) and flexural strength (78.9 MPa). Acoustic performance, which was determined through ASTM E1050-12, and the 50/50 hybrid was determined as the most effective sound absorber with a peak coefficient of 0.75 at 1900 Hz. The Scanning Electron Microscopy analysis revealed that there was good dispersion of fibres and low voids in hybrid samples and this is one of the reasons why they exhibit better multifunctional behaviour. In general, the 50/50 SCB-RH composite has the best thermal, mechanical and acoustic performance and it has great potential in the application of insulation and noise control in the automotive and architectural industry.

Article History
Received : 13 August 2025
Revised : 21 November 2025
Accepted : 13 February 2026
Published : 30 June 2026

Keywords
Natural fibre composites
Sugarcane bagasse
Rice husk
Thermal conductivity
Sound absorption
Mechanical properties

1. Introduction

Natural fibre composites (NFCs) have received significant interest in recent years due to their sustainability, low environmental impact and applicability in lightweight engineering systems [1]–[3]. These materials possess good properties, such as high specific strength, biodegradability, and cost-effectiveness, that make them competitive with conventional synthetic fibre composites [2], [4]. Their inherent cellular and porous properties provide efficient thermal insulation and sound-damping, which are very attractive for acoustic panelling, automotive interiors, and building applications [5], [6]. Natural fibres such as sugarcane bagasse (SCB) and rice husk (RH) can exhibit good tensile behaviour, high stiffness, and high impact resistance when properly processed, further increasing their multifunctional use. The selection of SCB and RH as materials for hybrid composite development is based on their complementary physicochemical properties [7]-[8]. The cellulose, hemicellulose, and lignin content of sugarcane bagasse is 40-50 %, 25-30 %, and 20-25 %, respectively, forming a rigid network of fibres that enhances load-bearing capacity and adhesion with polymer matrices due to the high lignocellulosic content. Conversely, rice husk contains 15-25% amorphous silica, which confers it with high thermal stability and resistance to degradation at high temperatures [9]–[11]. When combined, these two fibres synergistically enhance thermal insulation, mechanical performance, and acoustic absorption, making SCB-RH hybrids promising candidates for multifunctional bio-composite applications [12]–[14]. Strong fibre-matrix interfacial bonding is a major issue in composite fabrication and directly affects the mechanical and acoustic properties of the final composite. As a result of the hydroxyl (-OH) groups on natural fibres, these fibres are susceptible to moisture and incompatible with hydrophobic polymer matrices [15]-[16]. To overcome this, chemical treatments such as alkaline (NaOH) treatment, silane coupling agents, or acetylation are used to improve interfacial adhesion and fibre dispersion in the matrix. It has been shown that alkali-treated sugarcane bagasse and rice husk exhibit improved tensile properties due to increased surface roughness, which enhances mechanical interlocking between the resin and the fibres [17]. In addition, the final strength, thermal insulation, and acoustic damping of the composite depend on the distribution of fibre particle sizes. Fine particulate reinforcement increases surface-area interactions, coarse particles increase bulk strength, and an optimal balance is required for the intended application [18]-[19].

Numerous studies have examined the acoustic potential of natural fibre composites owing to their porosity, biodegradability, and sustainability. A hybrid system of sugarcane bagasse and bamboo charcoal was reported by Sakthivel et al. [4], with enhanced sound absorption at mid-frequencies attributed to the porous architecture and good dispersion of fibres within the matrix. In a comprehensive analysis, Jang [3] reviewed various green materials and emphasised that factors such as thickness, flow resistivity, and surface morphology are directly related to acoustic absorption, particularly in lignocellulosic materials such as sugarcane bagasse and rice husk. Bagheri et al. [20] found that adding tea waste and nanoclay to a polypropylene matrix resulted in significantly improved high-frequency acoustic performance, suggesting the importance of filler synergy and compatibility with the matrix. Rachman et al. [21] used

*CORRESPONDING AUTHOR | Niresh Jayarajan | ✉ nireshjayarajan@unimap.edu.my

coconut fibres with citric acid to develop environmentally friendly acoustic panels, in which chemical modification enhanced surface bonding and absorption coefficients at higher frequencies. As stated in Azhar et al. [22], the type of fibre, the method of layering, and the density of the material play a crucial role in the frequency-dependent effectiveness of acoustic panels, and coir and kenaf fibres have positive damping characteristics. Bachtiar et al. [23] emphasised the lack of standardisation in correlating mechanical integrity and acoustic response across different natural fibre composites, indicating inconsistencies in material design methodologies. Meanwhile, Taban et al. [24] conducted a comparative study of coir and date palm fibre composites and concluded that low- and mid-frequency sound absorption is affected by fibre diameter, packing structure, and interfacial bonding.

Despite these improvements, most previous studies have considered either mechanical or acoustic characterisation in isolation and have typically employed single-fibre systems. Very few studies have been conducted on hybrid natural fibre composites, especially in the sugarcane bagasse-rice husk systems. This research addresses this research gap by evaluating the performance of SCB-RH hybrid composites and exploring ways to develop sustainable materials with multifunctional applications in structural acoustics, transportation, and building insulation. Given the need for thermally insulating yet acoustically efficient materials, there has been increased focus on the sound absorption properties of NFCs. The sound absorption coefficient is one of the most important parameters for assessing the sound attenuation of a given material within certain frequency ranges. Natural fibre composites have good sound-damping properties because their porous structure allows sound waves to scatter and dissipate energy. Furthermore, the thermal conductivity of NFCs is important for applications that require heat management; hence, it is widely used to evaluate their thermal performance using Lee's Disc Method. Past research on natural fibre composites indicates that these materials have lower thermal conductivity than traditional synthetic materials, as plant fibres are inherently porous.

This research aims to provide an overall understanding of the structural performance of sugarcane bagasse and rice husk composites, with an emphasis on their potential for sound-absorption applications. These composites can be used as an alternative to petroleum-based materials, as they can be optimised to provide the required structural integrity, thermal performance, and sound-damping capabilities, and made sustainable. The findings from this study will advance high-performance bio composites by offering insights into their feasibility for industrial-scale acoustic applications. Further investigation into fibre-matrix compatibility, long-term durability, and advanced fabrication methods will be essential to unlocking the full potential of these materials in next-generation engineering solutions. While there have been several studies on natural fibre composites, most have been conducted on single-fibre systems or on the separate evaluation of mechanical, thermal, and acoustic properties. Very limited work has been done on SCB-RH hybrid composites, and no previous study has systematically correlated the composite's microstructure with its combined tensile, flexural, thermal, and acoustic behaviour. The novelty of this work is in the optimisation of the SCB-RH compositions and determination of the contrasting chemistries of the cellulose-rich SCB and silica-rich RH on the stiffness, deformation behaviour, thermal insulation, and sound absorption in a single composite system. This integrated evaluation offers new insight into the multifunctional performance of agro-waste-based hybrid composites, filling an obvious gap in existing literature.

2. Materials and Methods

2.1 Fibre Preparation

Sugarcane bagasse is an agricultural-industrial by-product composed mainly of cellulose (40-50%), hemicellulose (25-30%), and lignin (20-25%). The porous structure and high aspect ratio of SCB fibres enhance their sound-absorption properties, so SCB fibres have applications in acoustics. The lignin content provides moisture resistance and thermal stability, conferring advantages for acoustically active panels in various environmental conditions. Nevertheless, raw SCB fibre is hydrophilic due to the presence of hydroxyl (-OH) groups in its structure, and, therefore, it poses a problem of compatibility with hydrophobic polymer matrices. The adhesion and interaction between fibres and the matrix were enhanced by modifying the SCB fibre surfaces, such as through alkali treatments and silane coupling [25].

Figure 1. Fiber preparation

Rice husk is a natural reinforcement material with a high silica content (15-25%), hence it has high thermal insulation, flame resistance, and dimensional stability [26]. RH is a good addition to acoustic composites because its microporous structure enhances sound absorption. Its hard outer shell and micro-scaled particles contribute to the increased interfacial area in the composite, increasing the contact between the matrix and fibre. Moreover, the thermal conductivity of RH is low (0.035-0.045 W/mK), which facilitates heat insulation and decreases the chances of thermal degradation in composite panels. Nevertheless, it is brittle; thus, the fibre-matrix ratio must be optimised to balance structural integrity and acoustic performance. Figure 1 shows the process of fibre preparation. The matrix material used to bond the SCB and RH fibres

is a thermosetting resin system that provides support and additional acoustic damping. The resin used, as shown in the uploaded images, has sufficient integrity and some flexibility, allowing sound waves to dissipate. The hardener has been chosen to provide the required crosslinking and polymerisation, thereby improving the composite and enhancing resistance to environmental degradation [27]. Controlling the curing process improves adhesion between the fibres and helps reduce void formation, which is detrimental to maintaining uniform sound properties throughout the panel. The SCB and RH in different weights work well to optimise the mechanical strength, thermal insulation and acoustic damping properties. The fibrous morphology of the SCB increases the composite's porosity, thereby improving sound absorption by trapping air and reducing reflection. The microscale structure and silica-rich composition of RH provide sound attenuation through internal damping and reduced sound transmission. The two components, working in conjunction with an optimised resin-hardener system, permit the production of a composite that is lightweight, durable, and highly effective at providing sound absorption as acoustic panels for sound control in industrial or residential settings.

2.2 Composite Preparation

The sugarcane bagasse and rice husk materials used in the study were processed through several steps to enhance compatibility with the polymer matrix and improve acoustic characteristics [28]. First, the raw SCB and RH materials were washed with distilled water to remove contaminants, then dried at 80 °C for 6 h to remove any remaining moisture. After drying, the materials were ground in a high-speed ball mill and sieved to obtain an average particle size of 250–500 µm, promoting consistency and uniform distribution within the polymer matrix and thereby improving sound absorption. An alkaline treatment with a 5% NaOH solution was also carried out on the fibres to enhance interfacial adhesion with the epoxy resin and increase pore volume, thereby increasing acoustic damping. The treatment removed amorphous lignin and hemicellulose, increasing the fibre surface roughness and exposing more cellulose, thereby enhancing the mechanical interlocking capacity of the fibre and resin. The treated fibres were then repeatedly washed with distilled water to remove excess NaOH and placed in an oven at ambient temperature for 4 h to continue drying. The modified fibres exhibited enhanced wettability, hydrophobicity, and pore volume, thereby improving effective sound absorption. The composite preparation process is shown in Figure 2.

Figure 2. Composite preparation procedure

Table 1. Composition of composite panels and their sample code

Sample Code	Sugarcane bagasse (%)	Rice husk (%)	Epoxy resin (%)	Hardener (%)
Sample 1 ($S_{100}R_0$)	100	0	20	10
Sample 2 (S_0R_{100})	0	100	20	10
Sample 3 ($S_{70}R_{30}$)	70	30	20	10
Sample 4 ($S_{50}R_{50}$)	50	50	20	10
Sample 5 ($S_{30}R_{70}$)	30	70	20	10

The composite panels were fabricated using the hand lay-up technique to ensure uniform fibre distribution and minimise matrix impregnation. A thermosetting epoxy resin (bisphenol-A-based) accompanied by a polyamine-based hardener was utilised as the matrix. The per cent fibre-matrix ratios were kept in check by the formulation codes as provided in Table 1. To minimise fibre agglomeration and achieve uniform fibre distribution, the requisite amount of fibres was gradually added to the resin while stirring continuously. The mixture was poured into preheated moulds (200 mm × 200 mm × 5 mm) and vacuum-degassed to eliminate air voids, which were detrimental to acoustic performance.

The moulded panels were left to cure at room temperature for 24 hours and then post-cured for 2 hours at 60°C to increase the crosslinking density and the mechanical and acoustic properties of the resins. The cured composite sheets (Figure 3) were then cut into standard specimen sizes for sound absorption coefficient analysis, thermal conductivity, mechanical properties characterisation, and morphological analysis. In total, the five sample types changed the per cent composition of SCB and RH as listed in Table 1.

$S_{100}R_0$ S_0R_{100} $S_{70}R_{30}$ $S_{50}R_{50}$ $S_{30}R_{70}$

Figure 3. Prepared composite samples

2.3 Characterisation Techniques

The fabricated composite materials were subjected to a series of characterisation tests to evaluate their morphological, thermal, and mechanical properties. The characterisation methods used in this study are morphological characterisation by Scanning Electron Microscopy (SEM), thermal conductivity by Lee's Disc method, and mechanical testing to determine the tensile, flexural, and impact properties. Standardised testing protocols were followed to ensure reliability and reproducibility of the results. In accordance with ASTM standards, all mechanical and thermal characterisation tests were performed on 5 specimens of each composite type to ensure statistical accuracy and consistent performance evaluation.

2.3.1 Scanning electron microscopy

Scanning Electron Microscopy was used to assess the fibre distribution, fibre-matrix interface bonding, and fracture surface morphology of the composite samples. The samples were mechanically tested, and the examination was performed directly on their fractured surfaces without any conductive coating. Using this approach, natural fracture mechanisms, including fibre pullout, matrix cracking and interfacial debonding, were observed under realistic failure conditions. Qualitative evaluation of void formation, fibre breakage and matrix fibre compatibility critical to describing the mechanical behaviour of the composites was performed with the aid of SEM imaging [30]. In accordance with ASTM E766 [31], the procedure for visual inspection of fracture surfaces of composite materials, the analysis was performed. The direct examination was useful for assessing the effectiveness of fibre reinforcement and the dependence of microscale structural integrity on SCB-RH ratios.

2.3.2 Thermal conductivity test

The thermal conductivity (k) of the composite materials was measured using Lee's Disc Method, a widely accepted method for assessing the heat transfer characteristics of insulating materials, as shown in Figure 4. The apparatus consisted of a brass disc, a heating section, and thermocouples to evaluate steady-state heat transfer through the composite sample. The specimens were prepared in accordance with the standard test method ASTM E1952 [32], which describes a method for measuring the thermal conductivity of insulating materials. The experimental data were used to evaluate the composites' intended use in sound absorption applications by assessing their ability to limit heat transfer, an important aspect of acoustic damping performance.

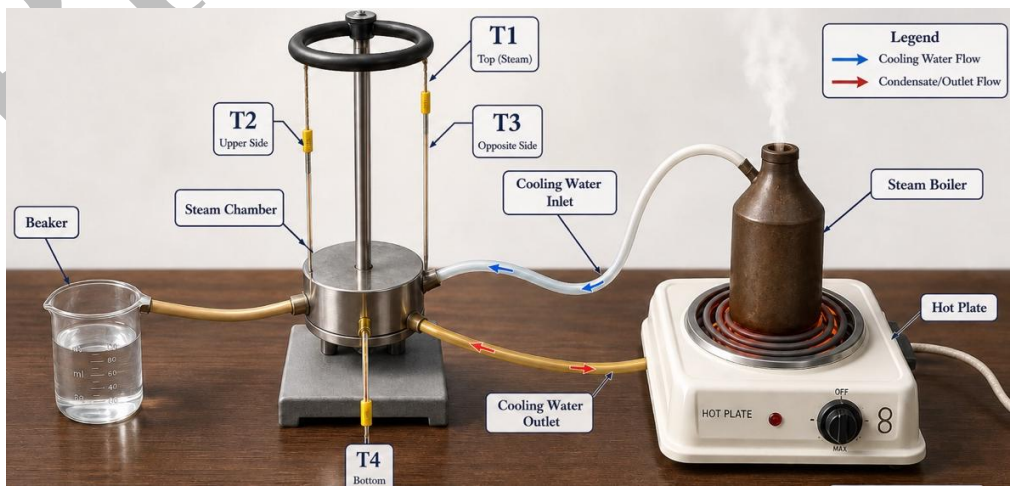

Figure 4. Lee's Disc method experimental setup

2.3.3 Mechanical testing

The mechanical performance of the composite samples was evaluated by tensile, flexural and impact tests in accordance with internationally accepted standards. Starting with tensile tests, tensile strength, Young's modulus, and elongation at break were determined using a Universal Testing Machine (UTM) in accordance with ASTM D638 [33] for polymer composites. Dog-bone specimens were prepared for the test, which was conducted at a constant strain rate up to failure to determine the stress-strain behaviour. Flexural strength and modulus of the composites were measured using a three-point bending test, according to the ASTM D790 [34] standards. This test subjected the material to a load applied at the centre, with both ends supported, to determine the composite's resistance to bending deformation. The Charpy impact strength of the composites was determined using an impact testing machine in accordance with the procedure of ASTM D256 [35]. Each material underwent a notched pendulum impact test to measure energy absorption under sudden loading, which is pertinent to toughness and shock resistance in acoustic applications. The data obtained through mechanical testing provide an overall range of structural, thermal, and mechanical performance of sugarcane bagasse and rice husk composites, highlighting their potential for sound absorption and acoustic insulation.

3. Results and Discussion

3.1 Thermal Conductivity Results

The thermal conductivity (K) of the composite samples was measured using the Lee Disc Method, a popular technique for low-conductivity materials. The technique is particularly appropriate to the study of composite materials derived from natural fibres, e.g. sugarcane bagasse and rice husk, due to their low thermal conductivity. This method presupposes that heat conduction in the sample is evenly distributed and that the thermal conductivity can be measured. A steady-state condition occurs when the temperature difference across the sample does not vary with time, making the measurements reliable. The thermal conductivity was calculated using the following equation:

$$K = \frac{mc(T_2 - T_1)}{A(t_2 - t_1)} \tag{1}$$

In equation (1), m represents the mass of the disc in kg, c denotes the specific heat capacity of the material in J/kg·K, ($T_2 - T_1$) indicates the temperature difference between the upper and lower surfaces in K, A refers to the cross-sectional area of the composite sample in m², and ($t_2 - t_1$) represents the steady-state temperature difference over time in s.

3.1.1 Thermal conductivity of sample 1 ($S_{100}R_0$)

The thermal conductivity of Sample 1 ($S_{100}R_0$) was determined by using Lee's Disc Method. This test was the first thermal characterisation performed in this study and serves as a baseline for comparison with the other composite formulations. The results obtained from steady-state temperature measurements and corresponding time intervals are presented in Table 2. The thermal behaviour of this sample is mainly affected by porosity, density, fibre morphology and chemical composition. Sugarcane bagasse fibres have a highly porous structure with large air pockets that act as thermal insulators by reducing heat conduction. However, because of the lower packing density, the resulting voids enable convective heat transfer, which, together with the packing density, results in an overall moderate thermal conductivity. The chemical structure of sugarcane bagasse, which is primarily composed of cellulose (40-50%), hemicellulose (20-25%), and lignin (20-25%), also contributes significantly to heat transfer mechanisms. Thermal stability is caused by lignin, whereas conduction is caused by cellulose along the fibre orientation. Also, it could have a relatively low thermal conductivity due to the absence of silica, a major insulating material in rice husk. The secondary effect on thermal conduction is the composite matrix, which is a mixture of 20% epoxy resin and 10% hardener. Experimental measurements of the rate of temperature change (R) were obtained and are given in Table 2. The mean of R was obtained as 0.02496 K/s. This preliminary analysis will help elucidate the thermal characteristics of sugarcane bagasse-based composites, which will be compared with other formulations in subsequent analysis.

Table 2. Thermal conductivity calculation for sample 1 ($S_{100}R_0$)

S. No	Temperature (K)	Time (s)	Range (ΔT) (K)	Time (Δt) (s)	R (ΔT/Δt)
1	347	0	1.0	39.0	0.02564
2	346	39	1.0	35.0	0.02857
3	345	74	1.0	43.0	0.02326
4	344	117	1.0	38.0	0.02632
5	343	155	1.0	36.0	0.02778
6	342	191	1.0	34.0	0.02941
7	341	225	1.0	48.0	0.02083
8	340	273	1.0	45.0	0.02222
9	339	318	1.0	37.0	0.02703
10	338	355	1.0	54.0	0.01852
11	337	409	-	-	-
		Average R			0.02496

3.1.2 Thermal conductivity of S_0R_{100}

Sample 2 (S_0R_{100}), which is entirely made of rice husk, was measured, and its thermal conductivity (k) was found to be 0.01927 W/mK as shown in Table 3. The insulation properties of this formulation are far more favourable than those of the sugarcane bagasse sample. The primary reason for this improved thermal insulation is the high silica content (approximately 15-20%) in rice husk, which is well known for its ability to significantly reduce thermal conduction. Silica has an extremely low thermal conductivity (in bulk form, 0.14 W/mK) and is therefore a good material for establishing a thermal barrier within the composite structure. Moreover, the rice husk packing arrangement is more compact than the sugarcane bagasse packing arrangement, implying minimal internal air pores that reduce convective heat transfer. The amorphous silica particles present in the husk of rice enhance the insulation capacity of the material as phonons are scattered and hence break the flow of heat and form lower thermal conductivity. Although the composite matrix, consisting of 20 % epoxy resin and 10 % hardener, provides the material with some additional heat resistance, the natural characteristics of rice husk remain the primary determinant of the composite's overall thermal conductivity. The steady-state temperature values and their corresponding periods (Table 3) provide further evidence of a slow heat-transfer rate, consistent with the insulating properties of the rice husk. The calculated rate of temperature change (R) for this composite was 0.01927 K/s, indicating a slower thermal response. These results indicate that rice husk-based composites can be applied as sustainable, lightweight thermal-shielding materials for thermal insulation and heat-resistant structures.

Table 3. Thermal conductivity of sample 2 (S_0R_{100})

S. No	Temperature (K)	Time (s)	Range (ΔT) (K)	Time (Δt) (s)	R (ΔT/Δt)
1	337	0	1.0	34.0	0.02941
2	336	34	1.0	56.0	0.01786
3	335	90	1.0	52.0	0.01923
4	334	142	1.0	58.0	0.01724
5	333	200	1.0	54.0	0.01852
6	332	254	1.0	63.0	0.01587
7	331	317	1.0	48.0	0.02083
8	330	365	1.0	85.0	0.01176
9	329	450	1.0	42.0	0.02381
10	328	492	1.0	55.0	0.01818
11	327	547	-	-	-
		Average R			0.01927

3.1.3 Thermal conductivity of sample 3 ($S_{70}R_{30}$)

The thermal conductivity of Sample 3 ($S_{70}R_{30}$), a composite material comprising 70% sugarcane bagasse and 30% rice husk (RH), was determined using steady-state temperature measurements. The rate of temperature change (R) was determined to be 0.02536 K/s, and the thermal conductivity was calculated from it, as shown in Table 4. The thermal conductivity of this hybrid composite falls between those of pure sugarcane bagasse (Sample 1, $S_{100}R_0$) and pure rice husk (Sample 2, S_0R_{100}), indicating a combined influence of both materials. The silica content of rice husk plays an important role in limiting heat transfer by scattering phonons, thereby contributing to the material's thermal insulation. However, the dominant presence of sugarcane bagasse (70%) creates a relatively porous fibre structure that allows for some convective heat transfer, resulting in a higher thermal conductivity than that of pure rice husk. This combination results in a balanced packing density, and the insulating properties of the rice husk are offset by the conductive properties of the sugarcane bagasse. The 20% epoxy resin and 10% hardener matrix in this composite helps to ensure a uniform distribution of the fibres, but not as much as the fibres themselves regarding thermal conductivity. The steady-state temperature data and their corresponding time intervals (Table 4) further support these results, as the composite has a heat transfer rate faster than that of 100% rice husk but slower than that of 100% sugarcane bagasse.

Table 4. Thermal conductivity of sample 3 ($S_{70}R_{30}$)

S. No	Temperature (K)	Time (s)	Range (ΔT) (K)	Time (Δt) (s)	R (ΔT/Δt)
1	347	0	1	39	0.02564
2	346	39	1	35	0.02857
3	345	74	1	43	0.02326
4	344	117	1	38	0.02632
5	343	155	1	36	0.02778
6	342	191	1	34	0.02941
7	341	225	1	48	0.02083
8	340	273	1	45	0.02222
9	339	318	1	37	0.02703
10	338	355	1	54	0.01852
11	337	409	-	-	-
		Average R			0.02536

3.1.4 Thermal conductivity of sample 4 ($S_{50}R_{50}$)

The thermal conductivity of Sample 4 ($S_{50}R_{50}$), a mixture of sugarcane bagasse and rice husk (RH) of 50% each, was measured with an average rate of temperature change (R) of 0.01882 K/s. This composite has a lower thermal conductivity than pure sugarcane bagasse and a higher thermal conductivity than pure rice husk, due to the combined effects of fibre composition, silica content, porosity, and composite density. The 50% rice husk fraction, which contains amorphous silica (around 15 - 20%), strongly hinders the transport of phonons, forming a thermal barrier, which limits the transport of heat through the material. On the other hand, the 50% sugarcane bagasse content, with its highly porous fibrous structure, allows air entrapment for insulation while still allowing some convective heat transfer through the interconnected voids. This balanced combination makes the composite's bulk density higher than that of 100% sugarcane bagasse but lower than that of 100% rice husk, making the structure more compact, partially eliminating air gaps, and better controlling heat dissipation. The 20% epoxy resin and 10% hardener matrix provide structural integrity and some heat resistance, although their effect on thermal conductivity is secondary to the properties of the fibre components. The constant temperature and the change in heat flux (Table 5) indicate that the heat transfer rate is moderate, supporting the composite's intermediate thermal conductivity relative to the pure SCB and RH samples. This hybrid composite offers a trade-off between thermal insulation and mechanical stability by leveraging the silica-rich particles in rice husk and the porous cellulose-lignin structure of sugarcane bagasse. As such, it is well-suited for energy-efficient structural applications, including thermal shielding panels, lightweight automotive components, and eco-friendly building materials, where moderate heat resistance and sustainable material use are key considerations.

Table 5. Thermal conductivity of sample 4 ($S_{50}R_{50}$)

S. No	Temperature (K)	Time (s)	Range (ΔT) (K)	Time (Δt) (s)	R (ΔT/Δt)
1	347	0	1	41	0.02439
2	346	41	1	51	0.01961
3	345	92	1	55	0.01818
4	344	147	1	62	0.01613
5	343	209	1	57	0.01754
6	342	266	1	47	0.02128
7	341	313	1	55	0.01818
8	340	368	1	53	0.01887
9	339	421	1	57	0.01754
10	338	478	1	54	0.01852
11	337	532	-	-	-
		Average R			0.01882

3.1.5 Thermal conductivity of Sample 5 ($S_{30}R_{70}$)

Sample 5 ($S_{30}R_{70}$) composed of sugarcane bagasse and rice husk in the ratio of 30% and 70%, respectively, showed a thermal conductivity value corresponding to an average temperature change rate (R) of 0.01880 K/s, which is lower than the 50% SCB - 50% RH composite but higher than the pure rice husk. The lower thermal conductivity in this formulation is mainly attributed to the higher proportion of rice husk, which contains a greater amount of amorphous silica (about 15-20%). Silica is an insulating agent that acts as a thermal barrier, preventing heat conduction and increasing thermal resistance, thereby reducing heat conduction through the material. This high silica content is responsible for the scattering effects, which further hinder conduction pathways and reduce convective heat transfer. Additionally, the lower fraction of sugarcane bagasse in this sample leads to lower porosity and fewer air gaps, resulting in a denser composite framework that further reduces convective heat transfer. The 20% epoxy resin and 10% hardener matrix used in this composite contributes to the composite's structural integrity and makes a small contribution to heat resistance. The steady-state temperature distribution, as shown in Table 6, indicates a slower thermal response, confirming the better insulating properties of this hybrid composition compared with compositions with higher sugarcane bagasse content. By combining the fibrous lignocellulosic structure of sugarcane bagasse with the silica-rich rice husk particles, $S_{30}R_{70}$ achieves an optimal balance between thermal insulation and mechanical strength, making it a viable candidate for energy-efficient applications. This composite is well-suited for use in thermal barrier coatings, aerospace insulation panels, and lightweight eco-friendly construction materials where enhanced thermal resistance and durability are essential.

Figure 5 shows the differences in thermal conductivity among the 5 composite formulations, indicating the effects of the fibre composition, pore structure, and silica content on heat transfer. The highest thermal conductivity of Sample 1 ($S_{100}R_0$) is due to its sugarcane bagasse composition, which has an interconnected lumen structure with larger pores, allowing heat to flow through solid conductive channels with minimal internal convection. When rice husk was added to the matrix for samples 2 (S_0R_{100}) and sample 3 ($S_{70}R_{30}$), thermal conductivity was decreased due to the introduction of silica-rich fine particles, which disrupt the conduction of heat by phonons and subsequently interrupt continuity of the conductive pathways within the composite. Additionally, rice husk has the highest silica content in Samples 4 ($S_{50}R_{50}$) and 5 ($S_{30}R_{70}$), resulting in lower thermal conductivity due to the amorphous nature of the silica, which disperses heat away from the matrix and increases resistance to thermal transport. Rice husk also increases the density of the grain structure, thereby reducing air entrapment within the composite and the voids that can facilitate convective heat transfer.

Across all samples, the epoxy matrix contributes minimally to heat transport, acting mainly as a binder, while the fibre–matrix interface and the degree of fibre packing play decisive roles in determining the final conductivity. The gradual reduction in thermal conductivity with increasing rice husk content in Figure 5 confirms the insulating nature of silica-rich agricultural fibres and demonstrates how hybridisation can be used to tailor the thermal response of natural fibre composites for specific engineering applications. The temperature-time relationships of all samples, as illustrated in Figure 6, confirm the earlier conclusions that composites with greater additions of rice husks continue to lose heat at a much lower rate than those with lower additions. This results directly from lower thermal conductivities associated with high levels of rice husk content. Therefore, the evidence provided by both Figures 5 and 6 clearly indicates that increasing the ratio of rice husk to silica will provide systematically enhanced performance (in terms of thermal insulation).

Table 6. Thermal conductivity of sample 5 $S_{30}R_{70}$

S. No	Temperature (K)	Time (s)	Range (ΔT) (K)	Time (Δt) (s)	R (ΔT/Δt)
1	338	0	1	41	0.02439
2	337	41	1	41	0.02439
3	336	82	1	56	0.01786
4	335	138	1	57	0.01754
5	334	195	1	58	0.01724
6	333	253	1	50	0.02000
7	332	303	1	55	0.01818
8	331	358	1	61	0.01639
9	330	419	1	63	0.01587
10	329	482	1	55	0.01818
11	328	537	-	-	-
		Average R			0.01880

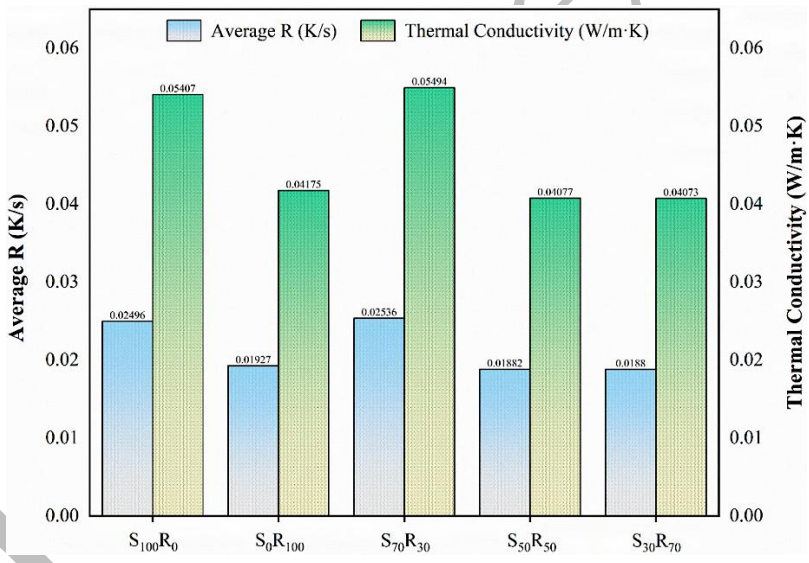

Figure 5. Thermal properties of hybrid polymer composite

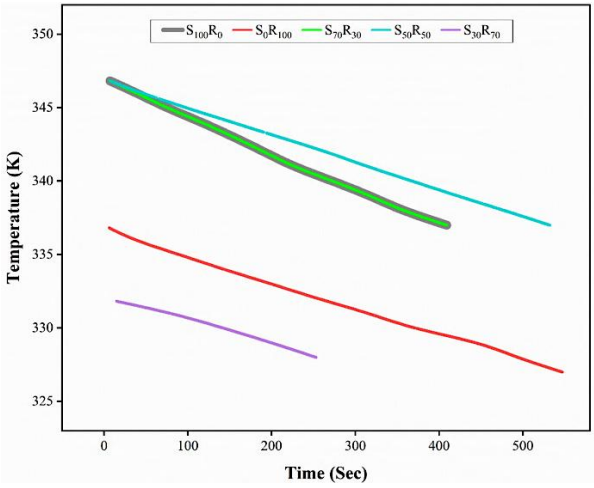

Figure 6. Temperature vs Time

3.2 Mechanical Properties

3.2.1 Tensile testing

Tensile characteristics of the composite specimens are largely influenced by the fibre composition, fibre-matrix interfacial adhesion and bonding, and the structural integrity of the polymer matrix. Sample 1 ($S_{100}R_0$) exhibited the lowest tensile strength (59.8 MPa), primarily because of the highly porous nature of sugarcane bagasse fibres, which provides less load-bearing capacity for the composite sample. SCB is composed mainly of cellulose (~40–50%), hemicellulose (~20–25%), and lignin (~20–25%), and the relatively lower lignin content in SCB reduces structural stability under tensile loading. Higher air voids and inconsistent fibre packing also limit stress transfer between the matrix and fibres, promoting earlier failure under tensile loading. Sample 2 (S_0R_{100}) exhibited a slightly higher tensile strength (69.6 MPa), largely due to the high silica content (~15–20%) in rice husk, which increases the stiffness and rigidity of the composite. However, despite greater structural integrity, the brittle nature of RH fibres limits flexural behaviour and energy absorption, thereby constraining improvements in tensile strength. Furthermore, although structural integrity is higher, the brittle nature of RH fibres limits flexural performance and energy absorption, thereby preventing an increase in tensile strength. Moreover, the poor interfacial bonding between RH and the epoxy matrix contributes to microstructural discontinuities, which tend to crack easily and exhibit low ductility, as seen in Figure 7, which shows the pre- and post-test conditions of the tensile specimens.

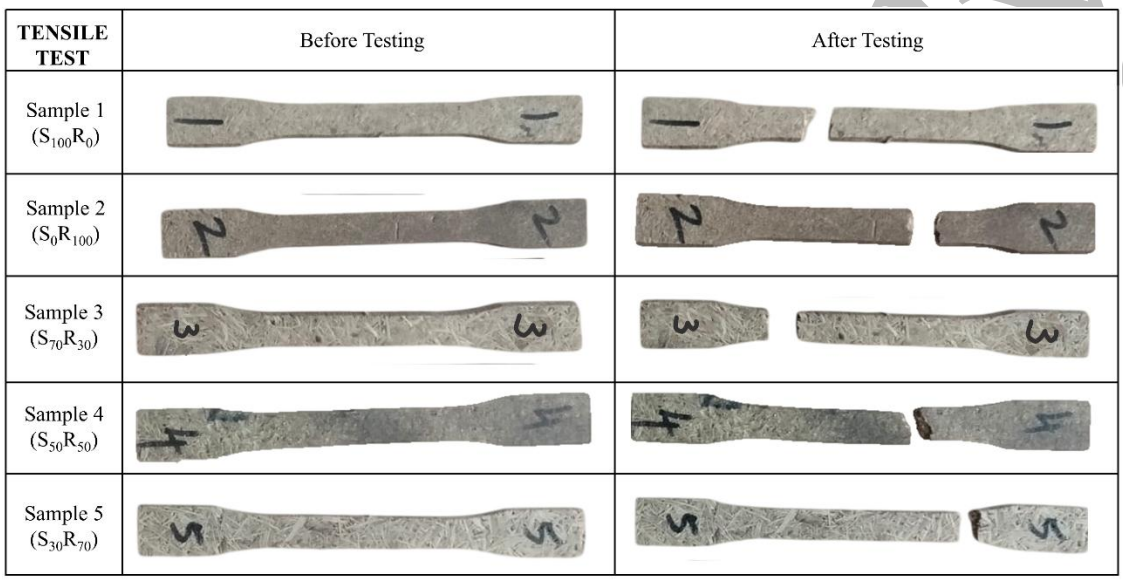

Figure 7. Before and after testing images of the tensile tested samples

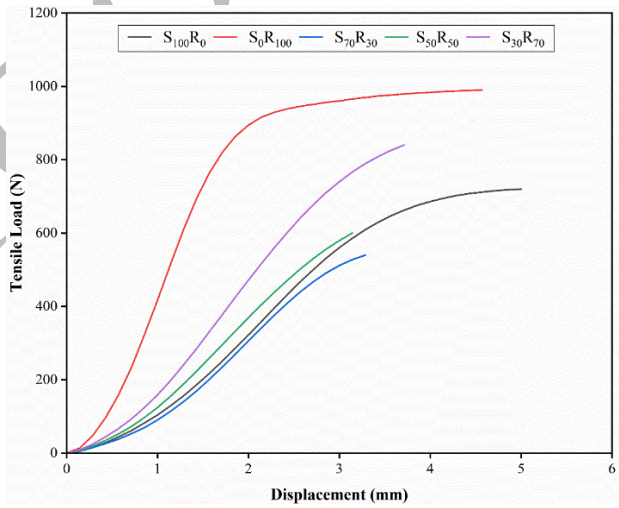

Figure 8. Tensile load vs displacement

The hybrid composites exhibited a significant increase in tensile strength due to the synergistic effect between sugarcane bagasse and rice husk fibres. Sample 3 ($S_{70}R_{30}$) indicated a tensile strength of 74.3 MPa, implying that the increased proportion of rice husk contributed to increased stiffness, while the presence of SCB contributed to ductility. Nevertheless, the high RH content imparted a microstructurally brittle nature and increased vulnerability to microcracking, which limited further tensile enhancement. Sample 4 ($S_{50}R_{50}$) had the highest tensile strength of 80.1 MPa, attributed to the optimal balance between the ductile behaviour of SCB and the rigidity of RH. This composition enabled it to distribute stress and transfer loads effectively within the matrix. This sample exhibited enhanced interfacial bonding,

which was more favourable for good fibre-matrix bonding, thereby minimising the potential for fibre pullout and failure under tensile loads. Sample 5 ($S_{30}R_{70}$) had a tensile strength of 77.7 MPa, which was though higher than $S_{70}R_{30}$, but lower than $S_{50}R_{50}$ due to the dominance of RH fibres. The high silica content in RH increased stiffness but reduced flexibility, thereby reducing energy absorption capacity under uniaxial stress. These findings affirm that hybridisation significantly outperforms single-fibre configurations, and that a 50:50 SCB–RH ratio offers the most effective combination of tensile strength, toughness, and structural integrity for advanced composite applications.

Table 7. Comparison of tensile and flexural properties with various hybrid polymer composite

S. No.	Literature	Composite Type	Tensile Strength (MPa)	Flexural Strength (MPa)
1	This Study	SCB-RH/Epoxy	80.1	78.9
2	[37]	Jute-Hemp/Polyster	26	70
3	[38]	PALF-Ramie fabric/Polypropylene	84.82	88.30
4	[39]	Jute-Glass fibre/Epoxy	90–110	120–150
5	[40]	Hemp–Flax/Epoxy	44.17	44.6
6	[41]	Sisal-Glass/Epoxy	70–100	100–140
7	[42]	Glass fiber-Rice husk/Epoxy	132.71	183

The mechanical behaviour of the composites is also illustrated by the load-displacement curve in Figure 8, which highlights the stiffness and deformation responses prior to tensile failure. The highest maximum load, 990 N, was recorded for sample 2 (S_0R_{100}), attributed to its high silica content and thick RH packing, which together contribute to high stiffness. Conversely, sample1 ($S_{100}R_0$) completely collapsed at 720 N because the SCB microstructure was porous, thereby restricting load transfer and reducing its resistance to deformation. Hybrid samples showed an intermediate response, with the best values of 540 N in sample 3 ($S_{70}R_{30}$) and around 600 N in sample 4 ($S_{50}R_{50}$), and a more progressive load increase curve, indicating enhanced stress redistribution through balanced fibre hybridisation. When compared with previously reported natural-fibre polymer composites (Table 7), the tensile performance of the present SCB–RH hybrids is comparable to several established systems. The optimised sample 4 ($S_{50}R_{50}$) (80.1 MPa) approaches the tensile strength of the PALF–ramie/PP composite (84.82 MPa), falls within the lower range of jute–glass hybrids (90–110 MPa), and exceeds that of the hemp–flax/epoxy composite (44.17 MPa) and sisal–glass/epoxy systems in their lower range (70–100 MPa). Although glass fibre–rice husk hybrids exhibit significantly higher tensile and flexural strengths due to the presence of synthetic reinforcement, the present SCB–RH natural-fibre hybrids demonstrate competitive mechanical performance within the natural-fibre composite category. This confirms that fibre hybridisation is an effective strategy for improving strength and stiffness through complementary interactions between the fibres.

3.2.2 Flexural testing

The flexural properties of composite samples were tested in accordance with ASTM D790. This standard specifies the method for determining the flexural strength, flexural modulus, and resistance to deformation of the material under bending loads. The test specimens were prepared as specified to ensure consistent fibre orientation and matrix distribution, so the results would not vary widely. Testing results indicate a strong correlation between flexural strength and factors such as fibre composition, interfacial bonding, and the material's ability to withstand bending loads before fracture. The maximum flexural strength of 78.9 MPa was recorded for sample 4 ($S_{50}R_{50}$), attributed to a balanced combination of SCB and RH that improved stiffness without compromising ductility. In contrast, Sample 1 ($S_{100}R_0$) had the lowest flexural strength of 60.40 MPa, likely due to the porous structure of SCB, which provides weaker structural integrity and reduced resistance to bending loads. Among the hybrid composites, sample 3 ($S_{70}R_{30}$) showed a flexural strength of 70.20 MPa, with an increase in RH content leading to increased rigidity but also brittleness. Sample 5 ($S_{30}R_{70}$) recorded a flexural strength of 68.26 MPa, indicating that an increased SCB ratio begins to reduce stiffness, although the presence of RH still contributes to structural performance. These results emphasise the role of fibre hybridisation in the design of flexural performance. A balanced composition can optimise the resistance to bending stress while maintaining structural integrity, making such composites promising for structural and semi-structural applications. The fracture behaviour and bending response before and after flexural testing are shown in Figure 9, further confirming the mechanical differences between the compositions.

The flexural behaviour of the composites, as shown in Figure 10, reflects the stiffness and failure behaviour, which are controlled by the fibre composition and microstructural packing. Sample 2 (S_0R_{100}) shows the sharpest load-displacement response, reaching a peak of 209.8 N at around 9.8 mm, indicating high stiffness due to the silica-rich rice husk. Its dense particles resist mid-span deflection and promote rapid load build-up. Sample 1 ($S_{100}R_0$), in contrast, has a much gentler response, reaching a comparable displacement at a peak load of only about 150 N at about 20 mm, which is attributed to the highly porous lumen structure of SCB resulting in the reduction of the bending rigidity and the improvement of compliance to flexural strains. The hybrid composites have mediocre but composition-related reactions. Sample 3 ($S_{70}R_{30}$) approaches approximately 419 N at around 9.8 mm, but failure occurs sooner due to greater brittleness and microcrack formation caused by the higher RH level. Sample 4 ($S_{50}R_{50}$) shows a more gradual and consistent load increment, reaching approximately 598–600 N at around 9.2–10 mm, demonstrating better crack bridging, stress rebound, and improved fibre–matrix compatibility due to the balanced SCB–RH ratio. Sample 5 ($S_{30}R_{70}$) reaches the maximum

flexural capacity, peaking at about 470 N at around 24.5 mm, where the prevalence of RH provides high stiffness and strong resistance to bending curvature, though at the cost of ductility after the peak.

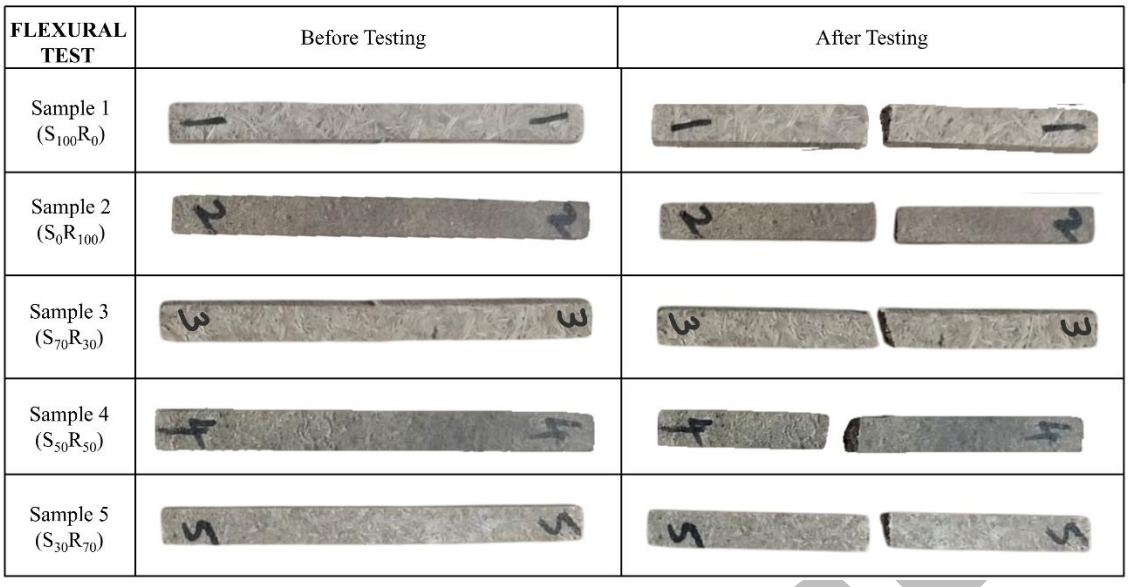

Figure 9. Before and after testing images of the flexural test samples

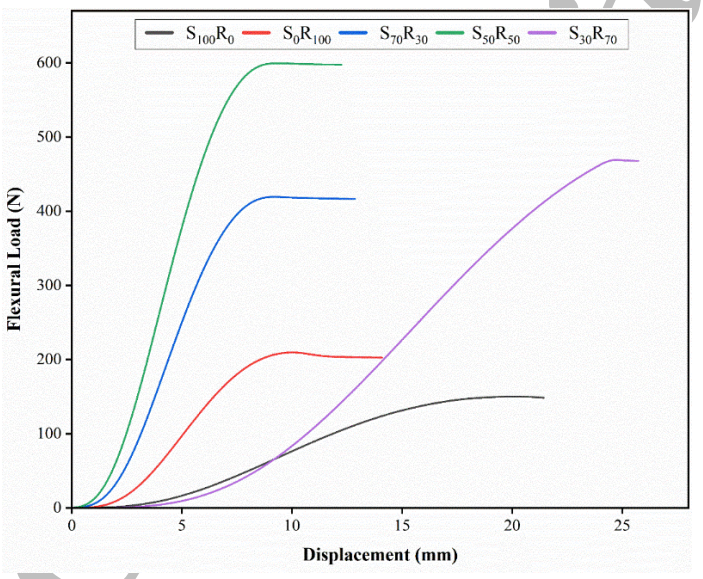

Figure 10. Flexural Load vs Displacement

The combined flexural curves support the statement that silica-based RH enhances stiffness and peak load, whereas SCB provides flexibility and deformation tolerance, and that tuned hybridisation allows flexural performance to be customised by controlling rigidity, fibre packing, and crack propagation. When the flexural strengths obtained in this study are compared with previously reported natural-fibre composite systems (Table 7), the SCB–RH hybrids demonstrate competitive performance within the category of fully bio-based composites. The optimised hybrid S70R30, with a flexural strength of 80.3 MPa, approaches the value reported for PALF–ramie/PP composites (88.30 MPa) and clearly exceeds that of hemp–flax/epoxy composites (44.6 MPa). The balanced S50R50 sample (78.9 MPa) also falls within the upper range of natural-fibre systems, although both SCB–RH hybrids remain below the flexural capacities of jute–glass (120–150 MPa) and sisal–glass hybrids (100–140 MPa) due to the absence of synthetic glass reinforcement in the present study. Although glass fibre–rice husk hybrids exhibit markedly higher flexural strength (183 MPa), the present SCB–RH composites fall squarely within the natural-fibre composite range and outperform systems such as hemp–flax, confirming the mechanical benefits of combining silica-rich RH for stiffness with SCB for deformation tolerance. This comparison highlights that natural-fibre hybridisation alone can achieve structurally meaningful flexural performance without synthetic reinforcement.

3.2.3 Impact testing

The impact properties of the composite samples were put to the test according to the ASTM D256 Standard Test Methods of Determining the Izod Pendulum Impact Resistance of Plastics. This test method provides an indication of a material's capacity to absorb shock loading and energy before fracture. Sample 4 ($S_{50}R_{50}$) had the highest impact resistance of 3.2

kJ/m^{2,} attributed to the effective energy dissipation provided by the sugarcane bagasse fibres and the structural rigidity of the rice husk. Sample 5 ($S_{30}R_{70}$) had an impact resistance of 2.9 kJ/m^2, indicating that the two fibres are good contributors to impact resistance, with an increase in SCB content facilitating energy absorption. Sample 3 ($S_{70}R_{30}$) had the lowest impact strength of 2.4 kJ/m^2, likely due to increased RH content, which leads to greater brittleness and reduced shock absorption. Sample 1 ($S_{100}R_0$) had an impact resistance of 2.1 kJ/m^2, indicating that although the porous structure of SCB is beneficial for energy absorption, it lacks the structural integrity to withstand fracture under abrupt loads. Sample 2 (S_0R_{100}) showed the lowest impact resistance of 1.8 kJ/m^{2,} attributed to RH being rigid and brittle, which led to faster crack propagation under impact. As summarised in Table 8, these findings indicate that the hybrid composite with a balanced or higher percentage of SCB exhibits greater toughness and is more suitable for applications requiring improved shock resistance. Figure 11 shows the progression of damage and the nature of fractures following impact testing, thereby substantiating the variations in toughness among the samples.

Table 8. Impact strength of composite samples

Sample Code	Composition (SCB/RH)	Impact Strength (kJ/m²)
Sample 1 ($S_{100}R_0$)	100% SCB	2.1
Sample 2 (S_0R_{100})	100% RH	1.8
Sample 3 ($S_{70}R_{30}$)	70% SCB + 30% RH	2.4
Sample 4 ($S_{50}R_{50}$)	50% SCB + 50% RH	3.2
Sample 5 ($S_{30}R_{70}$)	30% SCB + 70% RH	2.9

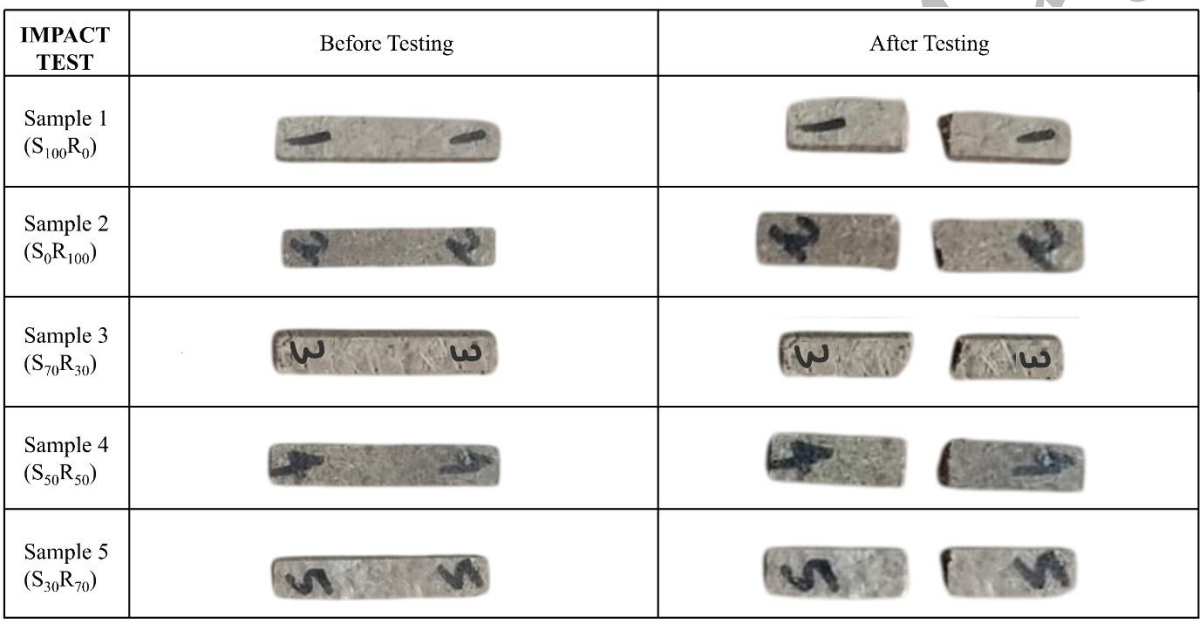

Figure 11. Before and after testing images of the impact test samples

3.3 SEM Analysis Results

The fractured surfaces of the composite samples are analysed using Scanning Electron Microscopy to provide useful information on microstructural properties, fibre-matrix adhesion, and failure mechanisms, as illustrated in Figure 12. The presence of a poor fibre-matrix interface means that adhesion between the reinforcement and the matrix is poor; therefore, stress transfer is reduced, and failure occurs early when the material is subjected to mechanical load. The interfacial adhesion is poor, allowing microcracks to develop that can propagate under applied loads, reducing the mechanical integrity of the composite. On the other hand, areas of good bonding indicate strong interfacial adhesion, contributing to mechanical performance through acceptable load sharing and limited stress concentration. The voids in the microstructure can be attributed to processing deficiencies or incomplete resin infiltration, which act as stress concentrators and decrease the strength and durability. Fibre pull-out may also indicate poor adhesion, as the reinforcing fibres are not adequately captured within the matrix, thereby reducing load-transfer performance. The observed microstructures are a plausible explanation for the mechanical test results: composites with better bonding exhibited greater tensile, flexural, and impact strength, whereas composites with interfacial defects showed lower performance due to premature failure mechanisms.

In addition to these observations of the microstructure, the SEM images show distinct failure behaviours across the different compositions. SCB-rich samples exhibit large fibre pull-out, collapsed lumens, and smooth fibre surfaces, suggesting that interfacial separation is the major failure mode due to the porous nature of SCB. RH-rich samples exhibit brittle fracture patterns, including sharp fibre breakage, microcrack branching, and clean fracture planes, which are attributable to the stiff, silica-rich morphology of RH. The hybrid composites exhibit mixed-mode failure, partial fibre pull-out, matrix shear, resin bridging, and fractured fibre bundles. Notably, Sample 4 (S50R50) shows fewer voids, tighter fibre packing and well-bonded fibre-matrix regions, which encourage crack deflection and delayed catastrophic failure.

These properties are strongly related to its improved mechanical performance, demonstrating that balanced fibre hybridisation increases failure resistance through enhanced interfacial adhesion and the stabilisation of crack propagation pathways.

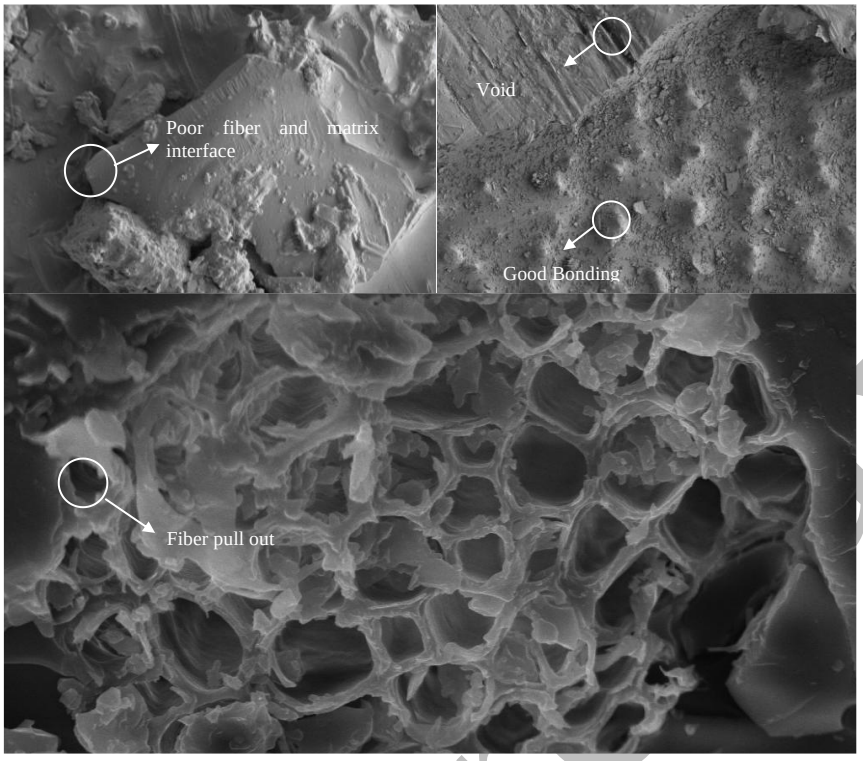

Figure 12. SEM results of prepared composites

3.4 Sound Absorbency Test

The normal-incidence sound absorption testing, in accordance with ASTM E1050-12, was conducted to assess the acoustic performance of the developed composites. An impedance tube was used to measure the sound absorption coefficient (a) over the frequency range 125 Hz to 6300 Hz. The findings were a clear indication that the fibre composition was a major factor influencing the absorption behaviour within the frequency bands under test. Sample 1 ($S_{100}R_0$), with high porosity due to its fibrous, loosely packed structure, showed very low absorption at low frequencies (alpha = 0.01 at 125 Hz) and a maximum of 0.24 at 3150 Hz. The random orientation of the SCB fibres improved internal reflection and extended the acoustic path, allowing mid-frequency damping. However, due to low structural stiffness and low surface impedance at higher frequencies, the composite was unable to maintain its absorption, with values decreasing beyond 4000 Hz. In contrast, Sample 2 (S_0R_{100}) with a denser and stiffer microstructure due to 15-25% silica content exhibited a progressive increase with frequency and reached its maximum value of 0.28 at 6300 Hz, as shown in Figure 13. This can be attributed to increased phonon scattering and reduced sound transmission, made possible by the rigid granular RH particles. However, its small pore volume and low airflow resistivity meant that it was not effective at low frequencies, where a was less than 0.08 up to 1000 Hz.

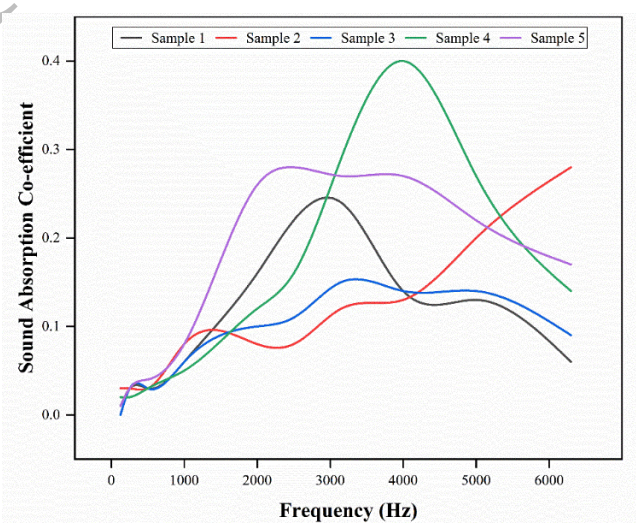

Figure 13. Sound absorption coefficient of various samples

The hybrid composites exhibited significantly enhanced broadband acoustic absorption, resulting from the synergy between the SCB and RH properties. Sample 3 ($S_{70}R_{30}$) with high RH content delivered rather flat and low absorption, with peak alpha only 0.15 at 3150 Hz, which means that too high RH decreased the number of interconnected voids and limited the viscous and thermal losses. Sample 4 ($S_{50}R_{50}$), with an equal balance of the two fibres, showed significantly better performance, with a peak alpha of 0.27 at 4000 Hz, as the SCB fibres provided air permeability and tortuosity, whereas RH provided stiffness for higher-frequency damping. Sample 5 ($S_{30}R_{70}$) showed the best acoustic performance, with a maximum absorption coefficient of 0.40 at 4000 Hz and maintained values above 0.27 across the frequency range of 3150-5000 Hz. The dominant SCB matrix enhanced internal friction and energy dissipation of multiple scattering paths in the porous structure, and the existence of RH enhanced impedance matching and reflection control at the material-air interface. The optimised interfacial bonding in hybrid samples further minimised reflection losses and improved energy absorption. These results highlight that adjusting the SCB-RH ratio directly affects the pore structure, airflow resistivity, and energy dissipation mechanisms, and that Sample 5 ($S_{30}R_{70}$) is the most acoustically efficient composite. Therefore, this formulation is especially suitable for engineering applications that require broadband sound insulation, such as acoustic wall panels, engine enclosures, or automotive interiors, where sustainable and high-performance materials are prioritised.

4. Conclusions

The detailed assessment of sugarcane bagasse and rice husk hybrid composites confirms that fibre composition is of paramount importance to the thermal, mechanical, and acoustic performance of the developed materials. Thermal conductivity testing showed that the lowest thermal conductivity was obtained for Sample 5 ($S_{30}R_{70}$), with a value of 0.04073 W/mK, due to the optimised combination of SCB porosity and RH stiffness, while Sample 1 ($S_{100}R_0$) showed the highest thermal conductivity (0.05407 W/mK) due to the porous structure of SCB. Among the hybrid configurations, Sample 4 ($S_{50}R_{50}$) achieved a balanced thermal conductivity of 0.04077 W/mK, indicating a synergistic insulating behaviour between the two fibres. Mechanical testing done as per the standards of ASTM D3039, ASTM D790 and ASTM D256 showed that Sample 4 ($S_{50}R_{50}$) had the best mechanical performance, with the highest tensile strength of 80.1 MPa, maximum flexural strength of 78.9 MPa and impact strength of 3.2 kJ/m^2. This was attributed to optimal fibre-matrix adhesion, improved stress distribution, and a balanced ratio of ductility from SCB and rigidity from RH. Acoustic testing under the ASTM E1050-12 standard confirmed that Sample 4 ($S_{50}R_{50}$) also exhibited the best sound absorption characteristics, with a peak sound absorption coefficient of 0.75 at 1900 Hz, attributable to its fibrous porosity and impedance-matching structure. The fractured surfaces of the samples were analysed by SEM, corroborating the results from the mechanical observations and showing better dispersion of the fibres, lower voids, and improved interfacial bonding in hybrid samples. These results make Sample 4 ($S_{50}R_{50}$) the most promising configuration with an optimal balance of thermal insulation, structural strength and acoustic damping. Consequently, this formulation is well-suited for multifunctional applications such as building acoustics, automotive panels, and thermal insulation systems, where lightweight, sustainable, and high-performance materials are especially important. Future investigations might extend this work by studying moisture resistance, long-term ageing behaviour, and environmental durability of SCB-RH composites under different humidity and temperature conditions. Further studies on surface modification of the fibre, resin optimisation, and nano-filler reinforcement may also improve mechanical stability and thermal-acoustic synergy. Additionally, investigation of fatigue response, recyclability and large-scale manufacturability would facilitate the wider application potential of these sustainable hybrid composites.

Acknowledgements

We would like to thank and acknowledge the Ministry of Higher Education Malaysia for financial support and Universiti Malaysia Perlis (UniMAP) for laboratory facilities and other related support for this project.

Funding

The authors would like to acknowledge support from the Fundamental Research Grant Scheme (FRGS) under grant number FRGS/1/2024/TK10/UNIMAP/02/7 from the Ministry of Higher Education Malaysia.

Declaration of Competing Interests

The authors declare no conflicts of interest.

Credit Authorship Contribution Statement

Niresh Jayarajan: Methodology, Data collection, Analysis, Writing – original draft
Tan Wei Hong –Conceptualisation; Supervision; Investigation; Validation; Writing-revise & review
Tamilselvan Ganesan: Methodology; Analysis; Validation; Writing-revise & review

Availability of Data and Materials

The data supporting this study's findings are available on request from the corresponding author.

Ethics Declarations

This study did not involve human participants or animals. Ethical approval was therefore not required.

Generative Artificial Intelligence Declarations

The authors claim that artificially intelligent-assisted technologies, such as generative AI, were not used to generate content, ideas, or theories. We have just utilised AI to enhance readability and refine the language. This was used with extreme human control and oversight. The authors take full responsibility for reviewing and approving the content.

References

[1] R. V. Patel, A. Yadav, and J. Winczek, "Physical, mechanical, and thermal properties of natural fiber-reinforced epoxy composites for construction and automotive applications," *Applied Sciences (Switzerland)*, vol. 13, no. 8, p. 5126, 2023. https://doi.org/10.3390/app13085126

[2] M. V. Khumalo, and S. Muniyasamy, "Bioplastics, Biodegradable Polymers and Biocomposites: An overview," in *Biodegradable Polymers, Blends and Biocomposites: Trends and Applications*, pp. 26-68, 2024. https://doi.org/10.1201/9781003304142-2

[3] E. S. Jang, "Sound absorbing properties of selected green material—A review," *Forests*, vol. 14, no. 7, p. 1366, 2023. https://doi.org/10.3390/f14071366

[4] S. Sakthivel, S. Senthil Kumar, E. Solomon et al., "Sound absorbing and insulating properties of natural fiber hybrid composites using sugarcane bagasse and bamboo charcoal," *Fibers and Fabrics*, vol. 16, p. 15589250211044818, 2021. https://doi.org/10.1177/15589250211044818

[5] A. Mehta, H. Vasudev, S. Singh et al., "Processing and advancements in the development of thermal barrier coatings: A review," *Coatings*, vol. 12, no. 9, p. 1318, 2022. https://doi.org/10.3390/coatings12091318

[6] S. F. Hashemi, M. Pourfallah, M. Gholinia, "Thermal performance enhancement in an indirect solar greenhouse dryer using helical fin under variable solar irradiation," *Solar Energy*, vol. 267, p. 112217, 2024. https://doi.org/10.1016/j.solener.2023.112217

[7] N. Jayarajan, T. W. Hong, T. Ganesan, "Performance evaluation of bamboo charcoal-filled natural fiber composites for sustainable structural and acoustic applications," *Building Acoustics*, vol. 32, no. 4, pp. 679-704, 2025. https://doi.org/10.1177/1351010X251371948

[8] S. A. Awad, O. Awayssa, M. Jawaid et al., "Performance enhancement of hybrid kenaf/bamboo Fiber-reinforced bio-epoxy composites for sustainable structural applications," *Journal of Materials Research and Technology*, vol. 41, pp. 29-38, 2026. https://doi.org/10.1016/j.jmrt.2025.12.017

[9] S. Dua, H. Khatri, J. Naveen, M. Jawaid et al., "Potential of natural fiber based polymeric composites for cleaner automotive component production - A comprehensive review," *Journal of Materials Research and Technology*, vol. 25, pp. 1086–1104, 2023. https://doi.org/10.1016/j.jmrt.2023.06.019

[10] S. P. Gairola, Y. Tyagi, and N. Gupta, "Mechanical properties evaluation of banana fiber reinforced polymer composites: A review," *Acta Innovations*, vol. 2022, no. 42, pp. 59-70, 2022. https://doi.org/10.32933/ActaInnovations.42.5

[11] D. F. Pereira, A. C. Branco, R. Cláudio, A. C. Marques, and C. G. Figueiredo-Pina, "Development of composites of PLA filled with different amounts of rice husk fibers for fused deposition modeling," *Journal of Natural Fibers*, vol. 20, no. 1, pp. 2162183, 2023. https://doi.org/10.1080/15440478.2022.2162183

[12] A. H. M. Ariff, T. T. Dele-Afolabi, T. H. Rafinet al., "Temporary sound barrier system from natural fiber polymeric composite," in *Materials Today: Proceedings*, 2022, vol. 74, pp. 438-449. https://doi.org/10.1016/j.matpr.2022.11.142

[13] O. J. Gbadeyan, T. P. Mohan, and K. Kanny, "Effect of loading nano-clay on banana fibers infused epoxy composite wear rate thermal property and water absorption properties," in *Materials Today: Proceedings*, 2023, vol. 87, pp. 252-256. https://doi.org/10.1016/j.matpr.2023.05.352

[14] D. Saber, A.H. Abdelnaby, and A.M. Abdelhaleim, "Fabrication of ecofriendly composites using low-density polyethylene and sugarcane bagasse: Characteristics' degradation," *Textile Research Journal*, vol. 93, no. 15–16, pp. 3666-3679, 2023. https://doi.org/10.1177/00405175231161281

[15] Y. Zhang, H. Wan, and B. Li, "Study on the thermal-oxidative aging performance of glass fiber reinforced epoxy composites," *Polymer (Guildf).*, vol. 334, p. 128707, 2025. https://doi.org/10.1016/j.polymer.2025.128707

[16] Z. Osman, M. Elamin, E. Ghorbel, and B. Charrier, "Influence of alkaline treatment and fiber morphology on the mechanical, physical, and thermal properties of polypropylene and polylactic acid biocomposites reinforced with kenaf, bagasse, hemp fibers and softwood," *Polymers (Basel)*, vol. 17, no. 7, p. 844, 2025. https://doi.org/10.3390/polym17070844

[17] T. Hassan, H. Jamshaid, R. Mishra et al., "Acoustic, mechanical and thermal properties of green composites reinforced with natural fiberswaste," *Polymers (Basel)*, vol. 12, no. 3, p. 654, 2020. https://doi.org/10.3390/polym12030654

[18] S. N. Yankevich, I. N. Khrol, and N. A. Kalinovskij, "Evaluation of the strength characteristics of polymer materials for the manufacture of personal electric vehicle elements," *Proceedings of the National Academy of Sciences of Belarus. Physical-technical series*, vol. 68, no. 1, pp. 24-31, 2023. https://doi.org/10.29235/1561-8358-2023-68-1-24-31

[19] A. Gani, M. Ibrahim, F. Ulmi, and A. Farhan, "The influence of different fiber sizes on the flexural strength of natural fiber-reinforced polymer composites," *Results in Materials*, vol. 21, p. 100534, 2024, https://doi.org/10.1016/j.rinma.2024.100534

[20] S. Bagheri, R. Jafari Nodoushan, and M. Azimzadeh, "Sound absorption performance of tea waste reinforced polypropylene and nanoclay biocomposites," *Polymer Bulletin*, vol. 80, no. 5, pp. 5203–5218, 2023. https://doi.org/10.1007/s00289-022-04295-y

[21] Z. A. Rachman, S. S. Utami, J. Sarwono, R. Widyorini, and H. R. Hapsari, "The usage of natural materials for the green acoustic panels based on the coconut fibers and the citric acid solutions," in *Journal of Physics: Conference Series*, 2018, vol. 1075, no. 1, p. 012048. https://doi.org/10.1088/1742-6596/1075/1/012048

[22] I. A. Azhar, K. Aini, M. Sari, "Comparison of sound absorption coefficient on natural fiber and recycle materials panel," *Progress in Engineering Application and Technology*, vol. 2, no. 1, pp. 225-233, 2021. https://doi.org/10.30880/peat.2021.02.01.021

[23] D. Bachtiar, Z. Zulfan, and A. Munawir, "Hybrid natural fiber polymer composites: A comprehensive review," *Jurnal Mekanova: Mekanikal, Inovasi dan Teknologi*, vol. 11, no. 1, pp. 169-18, 2025. https://doi.org/10.35308/jmkn.v11i1.11879

[24] E. Taban, A. Khavanin, M. Faridan, S. E. Samaei, K. Samimi, and R. Rashidi, "Comparison of acoustic absorption characteristics of coir and date palm fibers: experimental and analytical study of green composites," *International Journal of Environmental Science and Technology*, vol. 17, no. 1, pp. 39–48, 2020. https://doi.org/10.1007/s13762-019-02304-8

[25] V. P. K. de Maria, G. B. Torres, G. Dognani, R. J. dos Santos, F. C. Cabrera, and A. E. Job, "Sugarcane bagasse fiber as semi-reinforcement filler in natural rubber composite sandals," *Journal of Material Cycles and Waste Management*, vol. 21, no. 2, pp. 326-335, 2019. https://doi.org/10.1007/s10163-018-0801-y

[26] B. Haruna, I. Abdullahi, and U. Abdullahi, "A review on the use of agricultural and animal byproducts in polymer composites: a sustainable approach to materials reinforcement," *Journal of Engineering and Applied Science*, vol. 73, no. 1, p. 19, 2026. https://doi.org/10.1186/s44147-025-00862-y

[27] M. S. Oliveira, A. B. H. da S. Figueiredo, and S. N. Monteiro, "Ballistic energy absorption of thermally aged DGEBA/TETA system and fique-fabric reinforced epoxy composite," *Journal of Material Science and Technology Research*, vol. 10, pp. 94-101, 2025. https://doi.org/10.31875/2410-4701.2023.10.10

[28] N. Ibrahim, M. Jaafar, N. H. Che Hassan, and R. García Sanz, "Acoustic enhancement and weathering durability of rice Husk/PVC composites via microperforated design and nanocoating," *Journal of Building Engineering*, vol. 119, pp. 115253, 2026. https://doi.org/ 10.1016/j.jobe.2026.115253

[29] M. Mohammed, A. J. M. Jawad, A. M. Mohammed et al., "Challenges and advancement in water absorption of natural fiber-reinforced polymer composites," *Polymer Testing*, vol. 124, p. 108083, 2023. https://doi.org/10.1016/j.polymertesting.2023.108083

[30] A. E. Uzoma, C. F. Nwaeche, M. Al-Amin, O. S. Muniru, O. Olatunji, and S. O. Nzeh, "Development of interior and exterior automotive plastics parts using kenaf fiber reinforced polymer composite," *Eng*, vol. 4, no. 2, p. 1698-1710, 2023. https://doi.org/10.3390/eng4020096

[31] K. A. Bertness, "Dimensional measurement of nanostructures with scanning electron microscopy," *NIST Special Publication*, vol. 250, no. 96, 2017. https://doi.org/10.6028/NIST.SP.250-96

[32] American Society for Testing and Materials, *Standard Test Method for Thermal Conductivity and Thermal Diffusivity by Modulated Temperature Differential Scanning Calorimetry*, ASTM International, West Conshohocken, Pennsylvania, United States, 2008.

[34] American Society for Testing and Materials, *Standard Test Method for Tensile Properties of Plastics*, ASTM D638-14, ASTM International, West Conshohocken, Pennsylvania, United States, 2014.

[35] American Society for Testing and Materials, *Standard Test Method for Flexural Properties of Unreinforced and Reinforced Plastics and Electrical Insulation Materials*, ASTM D790-03, ASTM International, West Conshohocken, Pennsylvania, United States, 2015.

[36] American Society for Testing and Materials, *Standard Test Methods for Determining the Izod Pendulum Impact Resistance of Plastics*, ASTM D256-23e1, ASTM International, West Conshohocken, Pennsylvania, United States, 2023.

[37] M.Z. Islam, E. C. Sabir, M. Syduzzaman, "Experimental investigation of mechanical properties of jute/hemp fibers reinforced hybrid polyester composites," *SPE Polymers*, vol. 5, no. 2, pp. 192–205, 2024. https://doi.org/10.1002/pls2.10119

[38] L.F. Ng, M.Y. Yahya, C. Muthukumar, J. Parameswaranpillai, Q. Ma, M.R.M. Asyraf et al., "Swelling of lightweight pineapple leaf / ramie fabric-reinforced polypropylene hybrid composites," *Polymer (Guildf)*, vol. 16, no. 1847, 2024. https://doi.org/10.3390/polym16131847

[39] M.M. Hasan, M.A. Islam, T. Hassan, "Analysis of jute-glass fiber reinforced epoxy hybrid composite," *Heliyon*, vol. 10, no. 24, p. e40924, 2024. https://doi.org/10.1016/j.heliyon.2024.e40924

[40] K. Rasu A. Veerabathiran, "Performance of high strength natural fiber reinforced hybrid composites for structural engineering applications," *Materials Testing*, vol. 67, no. 3, pp. 553-560, 2025. https://doi.org/10.1515/mt-2024-0381

[41] J. Wagh, M. Madgule, S. Chaudhari, P. Deore, O. Deodhar, "Design and testing of flax-sisal-epoxy hybrid composites reinforced with glass fiber for automotive bumper beams," *Sigma Journal of Engineering and Natural Sciences – Sigma Mühendislik ve Fen Bilim. Derg*, vol. 56, no. 34, 2025. https://doi.org/10.14744/sigma.2025.1952

[42] B. Haruna, I. Abdullahi, U. Abdullahi, "A comprehensive review of performance enhancement of hybrid rice Husk polymer resin biocomposite," *Journal of Umm Al-Qura University for Engineering and Architecture*, vol. 16, no. 4, pp. 1-13, 2025. https://doi.org/10.1007/s43995-025-00167-4